Computers and Chemical Engineering 141 (2020) 106998

Contents lists available at ScienceDirect

Computers and Chemical Engineering

journal homepage: www.elsevier.com/locate/compchemeng

# NMPC-based control scheme for a semi-batch reactor under parameter uncertainty

Alex Kummer*, Lajos Nagy, Tamás Varga

*Institute of Chemical and Process Engineering, University of Pannonia, Veszprém H-8200, Hungary*

ARTICLE INFO

*Article history:*
Received 9 April 2020
Revised 4 June 2020
Accepted 27 June 2020
Available online 30 June 2020

*Keywords:*
Multi-Stage NMPc
Worst case scenario
Runaway criterion
Process safety
Parameter identification

ABSTRACT

Exothermic reactions are often performed in SBR because the generated reaction heat can be more easily kept under control in such construction. However, an unsuitable control system can lead to the development of thermal runaway, which may cause lethal damage. NMPC with implemented thermal runaway criteria is a promising tool to operate SBRs. However, engineers should always consider plant-model mismatch because uncertain predictions can cause undesirable scenarios. A novel control framework is proposed to operate SBRs and consists of NMPC with the implemented runaway criterion, extended Kalman filter and parameter identification algorithm. Both Multi-Stage NMPC and NMPC with the worst-case scenario are investigated and tested in terms of ability to handle parameter uncertainty. The former is 38 times slower than the latter with no noticeable increase in reactor performance. NMPC initialized based on the worst-case scenario with updating uncertain kinetic parameters results in a promising control structure for SBRs.



## 1. Introduction

Semi-batch reactors (SBRs) are widely applied for highly exothermic chemical reactions so operators can more easily keep the reactions under control. If one of the reagents is slowly fed to the other component(s), which is already in the reactor, the feed rate of reagents affects the heat evolution, so it can be controlled, and a suitable cooling system can be designed to remove the evolving reaction heat (Westerterp and Molga, 2004). For example, the oxidation of 2-octanol with nitric acid (van Woezik and Westerterp, 2000), Williams-Otto process (Rossi et al., 2016) and synthesis of lithium-etinolate are performed in semi-batch reactors.

The design of the reactor structure with all necessary components and the design of the operating strategy should be based on the mathematical model of the proposed system. The feeding trajectories are generally quite simple using a constant feeding rate over the entire process. Based on the initial conditions and properties of the reactor system, safe operating parameters can be defined with a constant feeding rate by calculating a safety boundary diagram (Zhang et al., 2019). A constant feeding rate can result in a higher batch time than a varying feeding rate during the operation. However, the constant feeding rate is necessary to keep the system in the safe operating regime if our information about the real processes contains uncertainties, which we do not address during the operation.

Moreover, engineers should always plan for plant-model mismatch, since it is difficult to obtain a model that describes the plant with sufficient accuracy. The plant-model mismatch can result in an undesirable event during the operation, and its prevention is necessary. Many methods can be found in the literature to handle this problem, such as considering uncertain parameters or applying state observers. Model Predictive Control (MPC) can provide a robust control approach to handle uncertainties of the system, where the feeding rate can be optimized. MPC is an advanced control system and can handle system boundaries (Rawlings and Mayne, 2009). An excellent review on the history of industrial MPC applications can be found in (Qin and Badgwell, 2003). Parameter uncertainty can be considered by applying the well-known min-max formulation (Kühl et al., 2007), multi-stage methods (Lucia et al., 2013), or tube-based methods (Mayne et al., 2005). Min-max MPC takes into account the worst-case realization of the parameter uncertainty, although it is conservative and may result in an infeasible optimization problem (Scokaert and Mayne, 1998). The conservativeness of min-max MPC was reduced by taking into

* Corresponding author.
*E-mail address:* kummera@fmt.uni-pannon.hu (A. Kummer).

https://doi.org/10.1016/j.compchemeng.2020.106998

**Nomenclature**

| | |
|---|---|
| c | concentration [kmol/m$^3$] |
| $c_p$ | heat capacity [Component A…G: kJ/kmolK; water: kJ/kgK] |
| d | reactor diameter [m] |
| e | control error |
| E | activation energy [kJ/kmolK] |
| F | feed rate [m$^3$/s] |
| $F_j$ | coolant feed rate [m$^3$/s] |
| h | reactor height [m] |
| i | ith scenario |
| I | runaway indication |
| k | kth time instance |
| $k_0$ | pre-exponential factor |
| MAT | maximum allowed temperature [°C] |
| n | moles [kmol] |
| N | number of scenarios |
| OP | controller output |
| p | parameters |
| PST | process safety time [s] |
| $PST_c$ | critical process safety time [s] |
| r | reaction rate [kmol/m$^3$s] |
| $r_c$, $r_T$ | partial derivatives of the reaction rate with respect to c and T |
| $S_p$ | component fraction of component "P" |
| t | time [s] |
| T | temperature [°C] |
| u | control input |
| U | heat transfer parameter [kW/m$^2$K] |
| RD | relative deviation |
| $q_{gen}$ | generated heat [kJ/s] |
| $q_{rem}$ | removed heat [kJ/s] |
| x | state vector |
| $x_{KC}$ | conversion of key component |
| V | reactor liquid volume [m$^3$] |
| $V_j$ | jacket volume [m$^3$] |
| w | weight factor |
| $\Delta H_r$ | reaction heat [kJ/kmol] |
| $\rho$ | density [kg/m$^3$] |
| $\rho^i$ | weight factor of ith scenario in PHA |
| $\lambda^i$ | weight factor of ith scenario in PHA |

*Subscripts*

| | |
|---|---|
| 0 | initial conditions |
| control | control horizon |
| C | cooling agent |
| dos | dosing |
| F | feed |
| dos | dosed |
| i | ith component |
| in,i | feed concentration of ith component |
| J | jacket |
| pred | prediction horizon |
| R | reactor |

account the future feedback information (Thangavel et al., 2018). Multi-stage MPC realizes the uncertainty by a tree of discrete scenarios, where each scenario must satisfy the predefined constraints (Lucia et al., 2013). Puschkle and Misos proposed a robust feasible multi-stage economic nonlinear model-predictive controller (eNMPC) with a heuristic multi-model approach, where the worst-case scenarios are generated based on sensitivities. They neglected the scenarios on the edges of the uncertainty set with low sensitivity (Puschke and Mitsos, 2018). A review of eMPC is found in (Ellis et al., 2014). Holtorf et al. presented Multi-Stage NMPC with on-line generated scenario trees that do not directly scale with the number of uncertain parameters (Holtorf et al., 2019).

In reactor operations, the first objective should always be the safe operation, especially when SBRs perform highly exothermic reactions, since a poorly designed reactor or poorly chosen operating parameters can lead to the development of reactor runaway. Although the phenomenon of thermal reactor runaway is well known, lethal accidents unfortunately still occurred in the recent past. The root cause of Seveso-disaster was thermal runaway in 1976 (Fabiano et al., 2017). In 2001, a polymerization reactor exploded because of a reactor runaway (Kao and Hu, 2002), and in 2007, an explosion occurred at T2 Laboratories, which caused the death of four people (Hall, 2010). Thermal runaway results in a rapid and significant temperature increase in the reactor, which can lead to explosion through the vaporization of reactants. The temperature increase in the reactor accelerates the heat generation because of the higher reaction rate, which further increases the temperature and may result in reactor runaway (Schweitzer et al., 2010). There are several runaway criteria, which classify the reaction operation states as runaway or non-runaway, so these equations can be applied to predict the development of thermal runaway (Kummer and Varga, 2019). Tailored runaway criteria were developed to obtain a more system specific critical equation (Kummer et al., 2019).

Adequate models of batch reactors can be used for a nonlinear model predictive control (NMPC) (Findeisen et al., 2007). Moreover, batch and semi-batch reactors that perform highly exothermic reactions can have highly nonlinear process dynamics, and the controller must cope with it. NMPC can be a suitable tool to handle nonlinear processes and is gaining more attention because it can capture detailed nonlinear dynamics of the system throughout the entire state space (Seki et al., 2001; Yu and Biegler, 2019). Since the goal of reactor operation is to maximize productivity while keeping the operation safe in the entire production time, prevention of thermal runaway is necessary. Thermal runaway criteria (Strozzi-Zaldivar and Modified Dynamic Condition) were implemented in NMPC to reliably indicate the development of runaway (Kummer et al., 2020).

Different stability analyses to predict the development of thermal runaway were successfully implemented in NMPC, such as the batch simultaneous model-based optimization and control (BSMBO&C) algorithm. This algorithm is an extension of NMPC and dynamic real-time optimization (DRTO) techniques, which use a Boolean term that penalizes the objective function when the controller system is close to thermal runaway (Rossi et al., 2015). Specific classes of deterministic NMPC/DRTO frameworks can identify reactor runaways under parameter uncertainty too (Rossi et al., 2017). Strozzi-Zaldivar criterion can be too strict; hence, it is not suitable to analyse the stability of semi-batch reactors in some cases (Kummer and Varga, 2017). Kähm-Vassiliadis criterion for exothermic batch reactors was introduced to overcome this problem, and the proposed stability criterion can be successfully applied in batch reactor control to perform highly exothermic reactions (Kähm and Vassiliadis, 2018a). This method was also successfully generalized to calculate with multiple reactions (Kähm and Vassiliadis, 2019). Their stability criterion was applied to an industrial case study and they considered the parameter uncertainty during the process control (Kanavalau et al., 2019). Lyapunov exponents as an indicator of stability were successfully realized in NMPC to control batch reactors (Kähm and Vassiliadis, 2018b). The operation of an industrial semi-batch polymerization reactor was optimized by considering a cooling system failure (Abel et al., 2000). The interaction between control and safety systems was also studied, where an LMPC (Lyapunov-based MPC) system was integrated with the activation of a safety system in a CSTR to avoid

thermal runaway (Zhang et al., 2018), and a good review about LMPC can be found in (Albalawi et al., 2018). Recently, two new NMPC-based methods were introduced to solve the closed-loop dynamic optimization problems, which were tested on a semi-batch reactor with potential runaway reactions, where the adiabatic temperature rise was considered to avoid reactor runaway. The first method is based on an adaptive backing off of their bounds along the moving horizon with a decreasing degree of severity. The second method is a chance-constrained control approach, which considers the relation between the uncertain input and the constrained output variables. Both methods consider the unexpected disturbances in advance, which results in a robust control approach (Arellano-Garcia et al., 2020).

We propose a control strategy for SBRs that perform potential runaway reactions, where the parameter uncertainty is considered. We consider the multiplicative uncertainty, so the model matrices are uncertain. The most crucial uncertainty sources from the reactor runaway viewpoint can be the kinetic parameters, heat transfer parameters and mixing efficiency for SBRs. The uncertainty in kinetic parameters is considered the source of model-plant mismatch in our work. NMPC with the embedded runaway criterion can be an effective tool to keep the reactor in the controllable zone, while the productivity is maximized. We investigated worst-case scenario and Multi-Stage NMPC to handle parameter uncertainty, although the computation cost of MS-NMPC is much higher. The goal is to develop a control framework for SBRs with exothermic reactions, which can be applied online in real reactor systems, so the computation time is critical. Therefore, we investigated the worst-case scenario with iteratively updating uncertain parameters by the least-squares method. NMPC naturally includes the model of the process, although the real process in this case is also a model. Our future work will be about implementing the proposed control scheme into a real laboratory reactor system. Currently, we can generate a plant-model mismatch to investigate the proposed control framework.

## 2. Proposed control structure of SBRs

This section will introduce the proposed general control methodology for SBRs that perform potential runaway reactions. The practical application of this control structure will be presented in Sections 3–4.

Our perspective is that using an NMPC with implemented runaway criterion can be an excellent solution to control SBRs, but we must handle parameter uncertainty to develop a reliable indication tool. The proposed control scheme for SBRs is shown in Fig. 1. When exothermic reactions occur in the reactor, the poorly identified kinetic parameters (or other model parameters) can easily lead to the development of thermal runaway in the application of the most appropriate criteria. In the proposed control scheme, the parameter uncertainty is handled by the combination of state estimation and a model identification algorithm. Since thermal runaway can have lethal consequence, the parameter uncertainty must be handled so that the probability of runaway is close to zero. For this purpose, Multi-Stage NMPC or worst-case scenario can be applied. Although we investigated Multi-Stage NMPC, its high computational cost is not encouraging (see Section 4.2.1); hence, we suggest applying the worst-case scenario with updating uncertain parameters (see Sections 4.2.2–4.2.3).

In Fig. 1, $u$ is the control inputs, $y$ is the reactor measurement outputs, $\bar{x}$ is the estimated states of the reactor, and $\bar{x}_i$ is the required estimated states for model parameter identification. This scheme is a general representation of the proposed control structure. In our case, $u$ consists of $OP_F$ *and* $OP_C$ (valve positions in the feed line and cooling agent line, respectively). $y$ includes $T_R$, $T_J$, and $V_L$ (reactor temperature, jacket temperature and liquid volume in the reactor). $\bar{x}$ consists of $\bar{c}, \bar{T}_R,$ *and* $\bar{T}_J$ (estimated concentration, reactor and jacket temperature, and reaction rate constants). $\bar{x}_i$ in our case includes $\bar{k}$ (reaction rate constants), and $p$ consists of $\bar{k}_0$ *and* $\bar{E}$, which are identified parameters. In the following sections, we introduce parts of the proposed control structure in more detail.

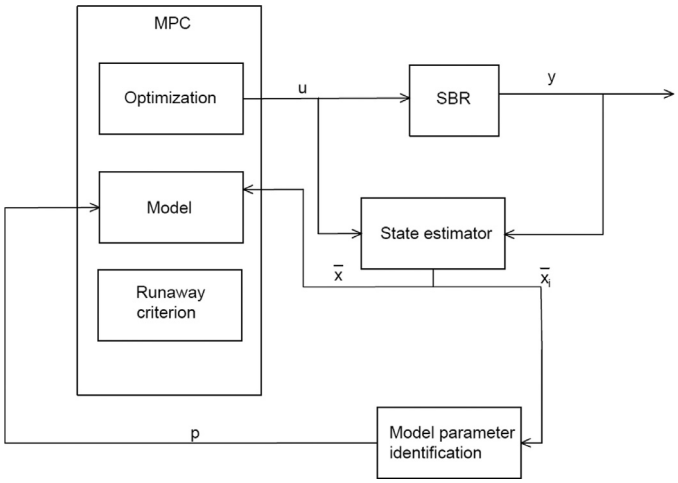


**Fig. 1.** Proposed control scheme for SBRs.

### 2.1. Temperature control of SBR

The main goal of the SBR operation is similar to any other kind of reactor or process unit, such as to maximize the productivity while keeping the reactor safe during the entire operation. The reactor temperature is controlled by manipulating the flow rate of feeding reagents (*TV001*) and cooling agent (*TV002*) into the reactor jacket, which is the often applied scheme. The control structure of the reactor system is shown in Fig. 2. The mass-flow of reagent feed is integrated, the amount of fed reagent is calculated ($V_{dos}$), and the liquid level is measured with LIT001. When the required reagent is added ($V_{dos,0}$), the reactor temperature control switches the actuator, and the temperature is controlled by manipulating the flow of cooling agent in the mixing phase, which was 80% of the total cooling capacity in the first phase of operation.

$$Actuator = \begin{cases} TV001 & V_{dos} < V_{dos,0} \\ TV002 & V_{dos,0} = V_{dos} \end{cases} \tag{1}$$

A safe operation is characterized by applying two safety regulations. One of them is a predefined Maximum Allowable Temperature (MAT), so the reactor temperature (TIT001) cannot exceed MAT. The other safety bound is applying a thermal runaway criterion to avoid dangerous runaway states. Runaway criteria classify runaway and non-runaway states based on the state variables and parameters of the studied process (concentration of reagents, process temperature, heat of reaction, heat transfer parameter, etc.). Therefore, avoiding runaway states increases the safety of the reactor operation. We applied the Modified Dynamic Condition (MDC) in the proposed control scheme (Kummer and Varga, 2019). The MDC states that the product of the increase in heat removal with increasing temperature and the generated to removed heat ratio must exceed the difference between the rate at which the heat generation increases as a result of an increase in temperature and the reduction in the reaction rate as a result of a decrease in reagent concentration. If the MDC is satisfied. the reactor states are considered non-runaway (i.e., normal) operation.

$$\left.\frac{\partial q_{gen}}{\partial T}\right|_c + \left.\frac{\partial m}{\partial c}\right|_T \leq \frac{dq_{rem}}{dT}\frac{q_{gen}}{q_{rem}} \tag{2}$$

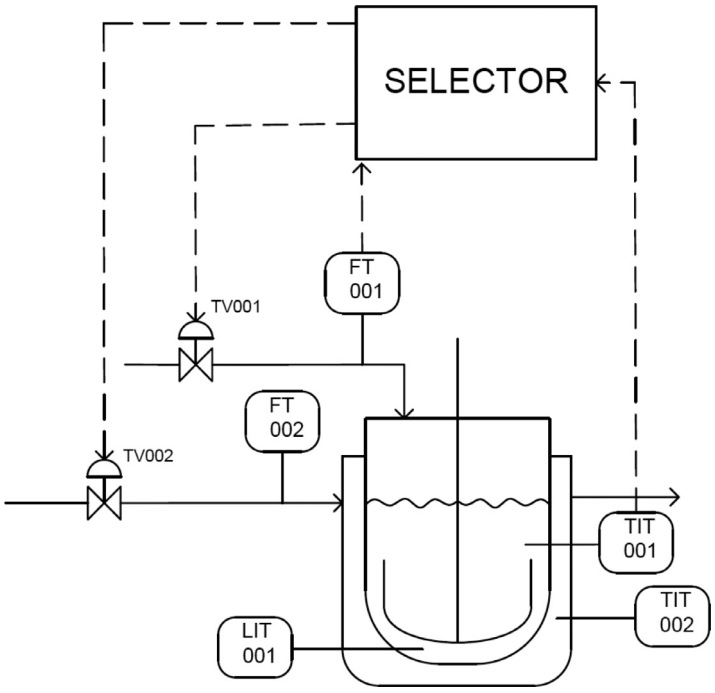


**Fig. 2.** Proposed control structure of SBRs.

where $q_{gen}$ is the generated heat in the reaction, $q_{rem}$ is the removed heat, and $m$ is a mass balance function.

Let us introduce variable $I(k)$ to evaluate the reactor operation based on runaway and non-runaway states. If Eq. (2). is satisfied, then $I(k) = 0$ (normal operation); otherwise, $I(k) = 1$ (runaway), where $k$ is the $k$-th time instance.

### 2.2. Open-loop optimization problem

The goal is to maximize the productivity while thermal runaway does not develop, so the conversion of the key component ($x_{KC}$) and selectivity for the product ($S_P$) are considered in the objective function next to the runaway states ($I_k$), and higher reactor temperatures than MAT ($e^+$) should be avoided. The objective function (or stage cost if we refer to Multi-Stage NMPC) is denoted by $L$, which represent a general cost function. The terms of the cost function are weighted ($w_x$, $w_s$, $w_u$, $w_I$, $w_T$), so a well performing control can be reached in different applications. In the third term in Eq. (4), significant changes in the manipulated variables are penalized.

$$e^+ = max\left(T_{R,k} - MAT; 0\right) \tag{3}$$

$$L = \; - w_x x_{KC} - w_s S_p + w_u |u_k - u_{k-1}| + w_I I_k + w_T e^+ \tag{4}$$

$$\min_{u_k} \sum_{0}^{t_{pred}} L(x_k, u_k) \tag{5}$$

which is subject to

$$x_{k+1} = f(x_k, u_k, d_k) \tag{6}$$

$$0 \le u_k \le 100\% \tag{7}$$

where $u_k \in R^{n_u} u_k$ is the control input (control valve), $n_u$ is the number of control inputs, each state ($x_{k+1} \in R^{n_x}$) is a function of the previous state ($x_k$), and $n_x$ is the number of states. The realization of uncertainty is denoted as $d_k \in R^{n_d}$, where $n_d$ is the dimension of the uncertainty vector.

### 2.3. NMPC to handle parameter uncertainty

We always must count on plant-model mismatch, so we must address the parameter uncertainty. This section introduces the formulation of Multi-Stage NMPC and Worst-case Scenario to handle this problem.

#### 2.3.1. Multi-Stage NMPC

Fig. 2 illustrates how the Multi-Stage NMPC works with the given horizon lengths. For Multi-Stage NMPC, combinations of maximal, minimal and nominal values of uncertain parameters are considered, which usually results in a robust behaviour of the controller (Thangavel et al., 2018).

Each path of the scenario tree is called a scenario and indicated as $i$, and it contains all states $x_k^j$ and control inputs $u_k^j$ of scenario $i$. The set of all occurring indices ($j$,$k$) is denoted by $T$ Lucia, 2014). The number of scenarios is introduced by $N$. The cost of each scenario is considered with the same weight, so the mean value of the costs will give the objective value. The formulation of Multi-Stage NMPC is shown in Eqs. (8)–((11).

$$\min_{u_k^j} \sum_{i=1}^{N} \frac{1}{N} \sum_{0}^{t_{pred}} L_i\left(x_k^i, u_k^i, d_k^i\right) \tag{8}$$

which is subject to

$$x_{k+1}^j = f\left(x_k^{p(j)}, u_k^j, d_k^j\right) \quad \forall (j, k+1) \in T \tag{9}$$

$$0 \le u_k^j \le 100\ \% \quad \forall (j,k) \in T \tag{10}$$

$$u_k^j = u_k^l \; if \; x_k^{p(j)} = x_k^{p(l)} \quad \forall (j,k), (l,k) \in T \tag{11}$$

where $x_k^{p(i)}$ is the parent node. To correctly represent the real-time decision problem, the control inputs cannot anticipate the values of the uncertainty that are realized after the corresponding decision point. It is important because it is not possible to give multiple input variations to the process at the current state (Puschke and Mitsos, 2018). This condition is enforced by Eq. (11), which represents

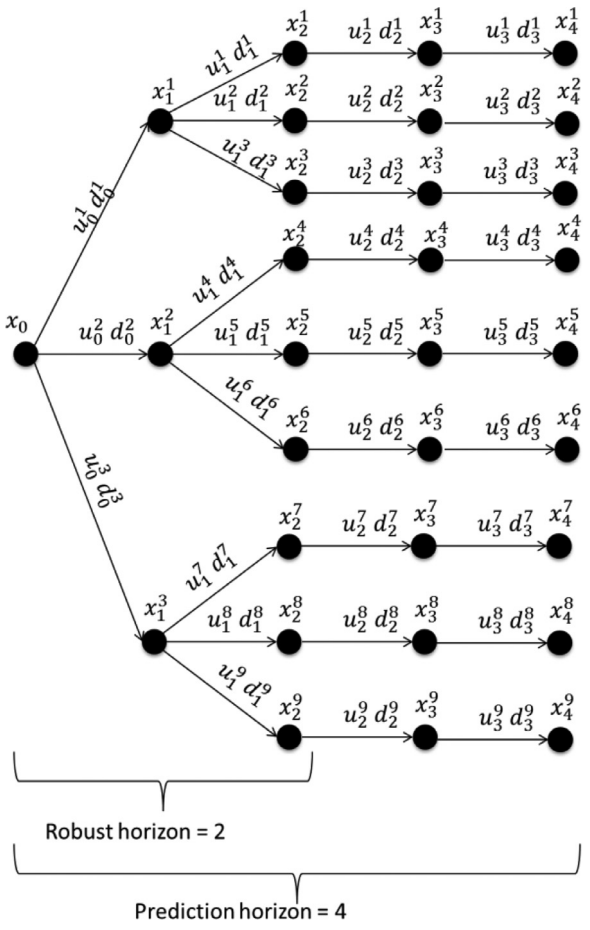


**Fig. 3.** Tree representation of the uncertainty evolution for a Multi-Stage NMPC (Thangavel et al., 2018).

the non-anticipativity constraints that require all control inputs at the same node to be equal. In Fig. 3, this condition implies that $u_0^1 = u_0^2 = u_0^3;\ u_1^1 = u_1^2 = u_1^3; \ldots$ [36].

The optimization problem was solved by the modified progressive hedging algorithm, which is a decomposition algorithm, where non-anticipativity constraints are relaxed by penalizing the difference between the control inputs that should satisfy the non-anticipativity constraints. Its advantage is that the scenarios can be independently solved, so the following Eqs. (12)–((15)) optimization problem must be solved. As shown by S. Lucia applying a longer robust horizon of one does not significantly improve the result, but it requires more computational effort, because the size of the optimization problem increases exponentially with it (Lucia, 2014). Since the length of robust horizon is one in this case, only the first control inputs ($u_0^i$) of different scenarios must satisfy the non-anticipativity constraint.

$$\min_{u_k^j} L_i\left(x_k^i, u_k^i, d_k^i\right) + \lambda^i\left(u_0^i - \hat{u}_0^i\right) + \rho^i\left(u_0^i - \hat{u}_0^i\right)^2 \tag{12}$$

which is subject to

$$x_{k+1}^j = f\left(x_k^{p(j)}, u_k^j, d_k^j\right) \quad \forall (j, k+1) \in T \tag{13}$$

$$0 \le u_k^j \le 100\ \% \quad \forall (j,k) \in T \tag{14}$$

$$\hat{u}_0^i = \sum_{i=1}^{N} \frac{1}{N} u_0^i \tag{15}$$

where $\hat{u}_0^i$ is the fictious value towards which the control inputs converge to satisfy the anticipativity constraints. Parameters $\lambda^i$ and $\rho^i$ are updated at each iteration to improve the convergence, where the update rule is:

$$\lambda^i = \lambda^i + \rho^i\left(u_0^i - \hat{u}_0^i\right) \tag{16}$$

$$\rho^i = min\left(\beta\rho^i, \rho_{max}\right) \tag{17}$$

where $\beta$ determines the increase of $\rho^i$. Eqs. (12)–(15) are iteratively solved until $max(u_1^i - \hat{u}_1^i) < \varepsilon$. After several iterations the non-anticipativity constraints are satisfied with desired tolerance $\varepsilon$.

### 2.3.2. Worst-case scenario

Two non-desired scenarios can be distinguished. In the first scenario, the reaction rate is much higher than expected; then, the generated heat will be much higher in the process than the model, which may cause thermal runaway. In the second scenario, the fed reagent accumulates because the reaction rate is lower than expected. When the concentration increases to a critical point, the reaction ignites, and thermal runaway may occur. To select the worst case scenario. we must choose between these two possible scenarios. There is a huge difference in ignition time between these two scenarios. The first scenario results in a more conservative solution, since the ignition time is lower; hence, if we can handle the first scenario, we can also avoid the second scenario. Therefore, we suggest kinetic parameters for worst cases that result in higher reaction rates, and we will apply the first scenario as the worst case by increasing the pre-exponential factor ($k_0$) and decreasing the activation energy ($E$) to the edge of the confidence interval.

## 2.4. Parameter identification

The logarithm of the reaction rate constant ($k$) linearly varies with the reciprocal of temperature (Eq. (18)), so the least squares method can be applied to estimate the pre-exponential factor and activation energy of the reaction.

$$ln\left(\bar{k}\right) = ln\left(\bar{k}_0\right) - \frac{\bar{E}}{RT} \tag{18}$$

Estimated reaction rate constants are required to calculate Eq. (18), so the state observer is necessary in the control structure. Since the reliability of the estimated kinetic parameters depends on the reliability of the state observer, we implement a condition that must be satisfied to overwrite the actual kinetic parameters.

$$RD = 100\frac{\sigma_p}{\mu_p} < 1\% \tag{19}$$

where $\mu_p$ and $\sigma_p$ are the mean and standard deviation of uncertain parameters. Due to this condition, the estimated kinetic parameters do not significantly vary, so our reliability in these parameters is higher. If the estimated parameters are far away from the worst case scenario the uncertain parameters are not updated. Therefore, we update these parameters if Eq. (19) is satisfied and if the estimated values are within the confidence interval.

## 2.5. State estimation based on the extended Kalman filter

In real systems only some measurements are available online (see Section 2.1), and usually each or none of the concentrations cannot be measured online. Therefore, state estimation of the system is necessary to use an effective NMPC in real systems. We must estimate the concentration of reagents and products and use it as a feedback in NMPC. The state estimation is necessary to

identify uncertain kinetic parameters. The extended Kalman filter is a suitable algorithm to estimate states of non-linear systems (Qu and Hahn, 2009; Khodadadi and Jazayeri-Rad, 2011), so we implemented this algorithm. If there is a closed-form expression for the predicted state as a function of the previous state ($\hat{x}_k$), controls ($u_k$) and noise ($w_k$), the predicted state is calculated by Eq. (20).

$$\hat{x}_{k+1} = f\left(\hat{x}_k, u_k, w_k\right) \tag{20}$$

The measurement is the function of the state ($x_k$) and measurement noise ($v_k$).

$$z_k = h(x_k, v_k) \tag{21}$$

Typically for SBRs, the measurement vector ($z_k$) consists of temperature and level measurements, and the state estimation vector $\hat{x}_k$ consists of concentrations and temperatures.

To improve the state estimation accuracy, additional variables were implemented into the model of EKF, which are the reaction rate constants of the reactions ($k_l$). Estimating new state variables in EKF is not time consuming, and it does not increase the computational time. To solve this issue, we must know how the reaction rate parameters vary with time; since the reaction rate parameter varies with temperature ($k = k(T)$), the following equation is defined:

$$\frac{dk_l}{dt} = \frac{dk_l}{dT}\frac{dT}{dt} = k_{0,l}exp\left(-\frac{E_l}{RT}\right)\frac{E_l}{RT^2}\frac{dT}{dt} \tag{22}$$

### 2.6. Process safety time to define the length of the prediction horizon

In case of MPC the prediction horizon must be sufficiently long to capture the first runaway states, so these states can be avoided during the reactor operation. Runaway criteria can be applied to define the length of prediction horizon by defining the first time instant when a runaway state occurs (also called the process safety time, PST) according to the applied runaway criterion. The PST can be defined as follows:

$$PST = argmin_k(I_k = 1) \tag{23}$$

Since the PST is a function of state variables and system parameters, we must calculate the PST for the worst case, which is called the critical PST. Thus, the SBR system must be considered a batch (i.e., if undesired events occur in SBRs, our first action should be closing the feeding valve of reagent), and we must calculate with those state variables where the probability of accumulation is the highest (low reactor temperature, initial reagents concentration, etc.). Different scenarios ($i = 1 \ldots n$) must be analysed by varying the initial concentration of reagents (which are fed into the reactor) to define maximum process temperatures ($T^{(i)}_{\max}$) and process safety times ($PST^{(i)}$). Critical initial states ($x_{0,c}$) will be these initial states where the maximum process temperature equals MAT. Length of prediction horizon will be the PST at critical initial states (Kummer et al., 2020).

$$t_{pred} = PST|_{i(T_{R,max}=MAT)} \tag{24}$$

## 3. Process model and analysis

This section presents the process model of the investigated fed-batch reactor from Williams-Otto process, where normal and abnormal operations that cause thermal runaway are presented. The process safety time of the system is also calculated to define the length of the prediction horizon.

### 3.1. Process model of the reactor system

The Williams-Otto process (WOP) has been used for years to test different control and optimization algorithms Arellano-Garcia et al., 2020). We optimize the fed-batch version of this process as presented in (Rossi et al., 2016). In the Williams-Otto process three exothermic reactions occur, which are presented in Eqs. (25)–((27) followed by the equation of reaction rates.

$$A + B \rightarrow C \qquad r_1 = k_{0,1}exp\left(-\frac{E_1}{RT}\right)c_A c_B \tag{25}$$

$$B + C \rightarrow P + E \quad r_2 = k_{0,2}exp\left(-\frac{E_2}{RT}\right)c_B c_C \tag{26}$$

$$C + P \rightarrow G \qquad r_3 = k_{0,3}exp\left(-\frac{E_3}{RT}\right)c_C c_P \tag{27}$$

Component $A$ is preloaded and component $B$ is continuously fed into the reactor. The desired product is component $P$, and two co-products can be formed: components $E$ and $G$.

The following differential equations Eqs. (28)–((31)) describe the dynamical behaviour of the reactor system:

$$\frac{dc_i}{dt} = \frac{F^{in}}{V_R}\left(c_i^{in} - c_i\right) + \sum_{l=1}^{N_R} \upsilon_{il} R_l \;\; i = 1 \ldots N_C \tag{28}$$

$$\frac{dV_R}{dt} = F^{in} \tag{29}$$

$$\frac{dT_R}{dt} = \frac{4U}{D_R \sum_{i=1}^{N_C} c_i cp_i}\left(T_j - T_R\right) + \frac{F^{in}\sum_{i=1}^{N_C} c_i^{IN} cp_i}{V_R \sum_{i=1}^{N_C} c_i cp_i}\left(T^{in} - T_R\right) - \frac{\sum_{l=1}^{N_R} \Delta H_{r,l} R_l}{\sum_{i=1}^{N_C} c_i cp_i} \tag{30}$$

$$\frac{dT_j}{dt} = \frac{4UV_R}{D_R V_j \rho_j cp_j}\left(T_R - T_j\right) + \frac{F_j}{V_j}\left(T_j^{in} - T_j\right) \tag{31}$$

The kinetic parameters, component properties and reactor constructional and operating parameters are summarized in Tables 1–3. The parameters will be handled as nominal hereinafter. The constraints are defined in Table 3, such as the MAT, and maximum feed rates of the reagent and cooling agent.

**Table 1**
Kinetic and thermodynamic parameters of reactions (Rossi et al., 2016; Sriram and Stevens, 1973).

| Parameter | | Value | Unit |
|---|---|---|---|
| Pre-exponential factors | $k_{0,1}$ | 1.3833 $10^5$ | $\frac{m^3}{kmol\ s}$ |
| | $k_{0,2}$ | 6.0098 $10^7$ | |
| | $k_{0,3}$ | 2.2288 $10^{11}$ | |
| Activation energies | $\frac{E_1}{R}$ | 6450 | $K$ |
| | $\frac{E_2}{R}$ | 8778.5 | |
| | $\frac{E_3}{R}$ | 11,155 | |
| Heat of reactions | $\Delta H_{r,1}$ | −1.851 $10^5$ | $\frac{kJ}{kmol}$ |
| | $\Delta H_{r,2}$ | −2.5765 $10^5$ | |
| | $\Delta H_{r,3}$ | −5.053 $10^5$ | |

**Table 2**
Component properties (Rossi et al., 2016; Sriram and Stevens, 1973).

| Component | Molecular weight [kg/kmol] | Specific heat [kJ/kmolK] |
|---|---|---|
| A | 142 | 321.204 |
| B | 60 | 127.14 |
| C | 202 | 352.288 |
| E | 81 | 166.212 |
| P | 181 | 426.617 |
| G | 383 | 844.132 |
| | | [kJ/kgK] |
| Cooling agent (water) | 18 | 4.186 |

**Table 3**
Reactor constructional and operating parameters (Rossi et al., 2016; Sriram and Stevens, 1973).

| Parameter | Value | Unit |
|---|---|---|
| d | 1 | M |
| h | 3.5 | M |
| $V_j$ | 0.8236 | $m^3$ |
| U | 0.8 | $\frac{kW}{m^2}$ |
| $c_{in}$ | 1 | $\frac{kmol}{m^3}$ |
| $T_{in,R}$ | 298 | K |
| $T_{in,j}$ | 298 | K |
| $c_{0,A}$ | 1 | $\frac{kmol}{m^3}$ |
| $V_0$ | 0.5 | $m^3$ |
| $T_{0,R}$ | 312 | K |
| $T_{0,J}$ | 308 | K |
| $F_{max}$ | 1e-3 | $\frac{m^3}{s}$ |
| $F_{j,max}$ | 1e-2 | $\frac{m^3}{s}$ |
| MAT | 335 | K |

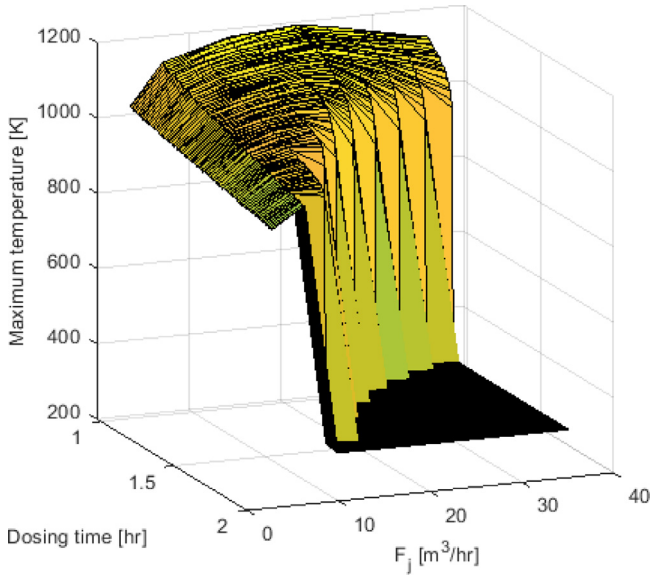


**Fig. 4.** Reactor behaviour at different dosing times and cooling agent flow rates.

### 3.2. Analysis of wop in SBR

The behaviour of the investigated reactor system was analysed with no control system (i.e., the B reagent feed is constant), where the maximum process temperatures are analysed in functions of the dosing time and flow rate of cooling agent. The remaining applied parameters are shown in Section 3.1. As shown in Fig. 4, poorly chosen operating parameters can develop thermal runaway. According to the model, the process temperature can exceed 900 K. The maximum temperature rapidly increases, and there is no interior point between normal process temperatures (under MAT) and runaway temperatures (>900 K). Although the optimal feeding trajectory can increase the productivity, increasing the flow rate of cooling agent enables an operation with less dosing time, as shown in Fig. 4.

Runaway states are distinguished by the MDC criterion, and the derived critical equation for the process is introduced in Eq. (32).

$$\sum_{l=1}^{nr} -\Delta H_{r,j} r_{j,T} V - \sum_{l=1}^{nr}\sum_{i=1}^{nc} r_{l,c_{li}} \leq \frac{\sum_{l=1}^{nr} -\Delta H_{r,l} r_l V}{T_R - T_j} \tag{32}$$

where *nr* is the number of reactions, *nc* is the number of reagents in the $L$-th reaction, $r_T$ and $r_c$ are the derivatives of the reaction rate with respect to temperature and concentration of reagents respectively.

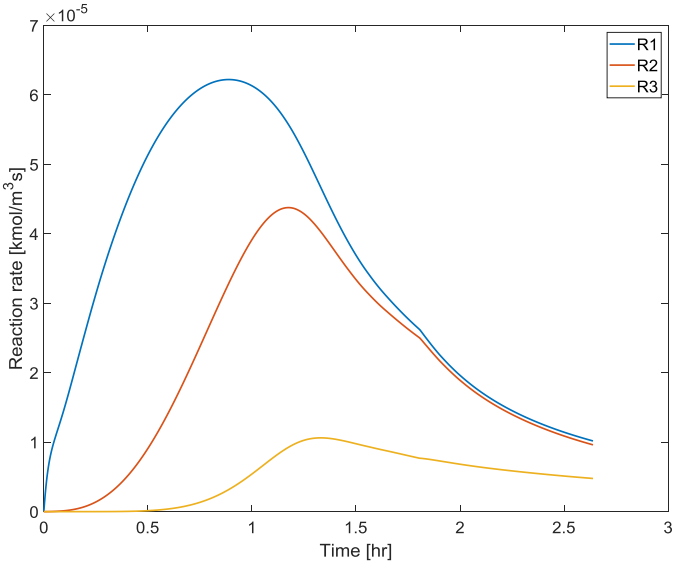


**Fig. 5.** Reaction rates during an operation (Dosing time: 1.8 hr, Feed rate: 0.55 $m^3$/hr, Cooling flow rate: 36 $m^3$/hr).

To avoid thermal runaway uncertain kinetic parameters are quite significant, so we investigate how the parallel reactions dominate during the reactor operation. Fig. 5 shows the reaction rates; the first reaction (R1) has the highest rate during the whole operation. To investigate the proposed control scheme, we only choose the kinetic parameters of the first reaction as uncertain. Because the first reaction is dominant, the uncertainty of this reaction has the highest effect on the behaviour of the reactor.

### 3.3. Process safety time of the system

As presented in Section 2.6, the length of the prediction horizon can be defined based on the process safety time of the system. Maximum reactor temperatures and PSTs are investigated, as shown in Fig. 6. MAT is reached at ~1.36 $\frac{kmol}{m^3}$ initial concentration, where the PST is 0.59 h. In this case, the minimum length of the prediction horizon is 0.59 h.

### 3.4. State estimation of the investigated system

This section presents the efficiency of EKF on the investigated model system. First Eqs. (28)–(31) were applied to estimate the states of the system, and the measured variables are the reactor temperature, jacket temperature and reaction volume (the inflow rate is measured, which is the only parameter that increases the reaction volume). The results are generated next to 5% parameter deviation in pre-exponential factor and activation energy of the first reaction.

As shown in Fig. 7a, the estimations of reagent concentration are quite poor, which can result in false runaway indication and thermal runaway of the system. If the first reaction rate parameter ($k_1$) is estimated the accuracy can be increased, as presented in Fig. 7b. The state estimations are acceptable with this modification.

## 4. Results of NMPC

This section provides the results of NMPC with and without parameter uncertainty. The performance improvement due to parameter identification is presented. The optimization problem was

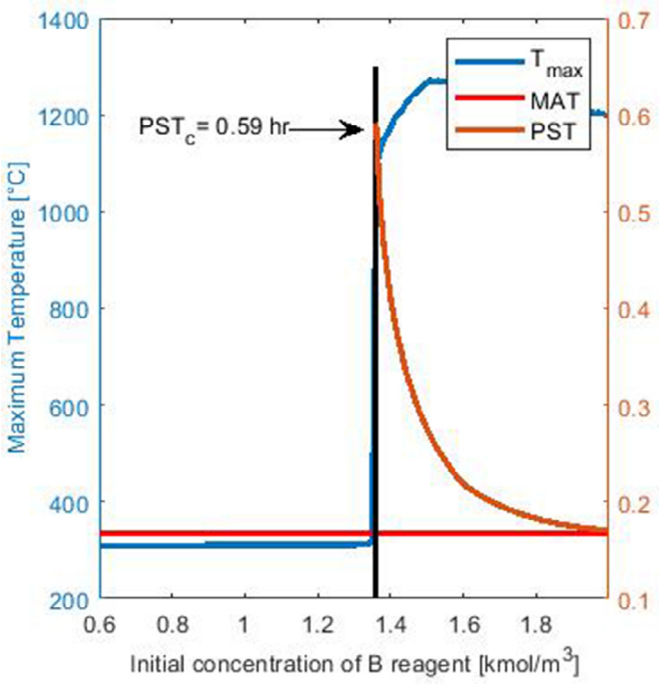


**Fig. 6.** PST of the system according to the MDC criterion.

**Table 4**
Parameters of NMPC.

| | | |
|---|---|---|
| Sample time | $T_0$ | 100 s |
| Prediction horizon | $t_{pred}$ | 2200 s |
| Control horizon | $t_{contr}$ | 500 s |
| Weight factor in Eq. (4) | $w_e$ | 500 |
| Weight factor in Eq. (4) | $w_u$ | 0.01 |
| Weight factor in Eq. (4) | $w_l$ | 100 |

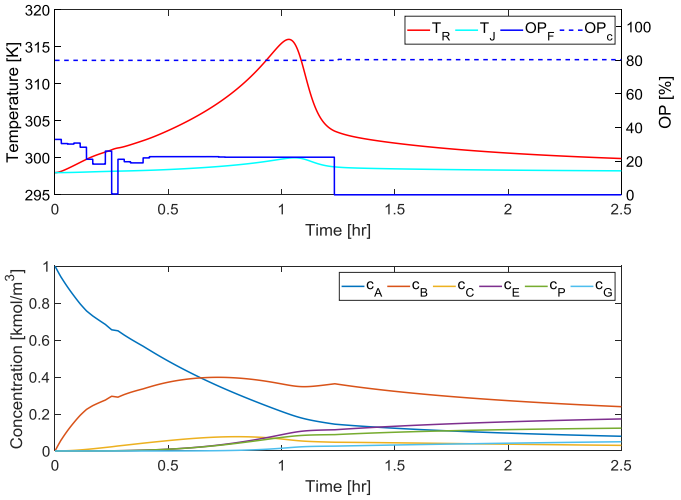


**Fig. 8.** Reactor operation with nominal NMPC.

solved by the interior-point algorithm, where the algorithm proceeds a moving horizon (Vanderbei and Shanno, 1999). The applied parameters, which were heuristically selected, are summarized in Table 4.

### 4.1. Results of the open-loop control without parameter uncertainty

NMPC is tested without any uncertain parameter and the results are shown in Fig. 8. The reactor temperature stays far below

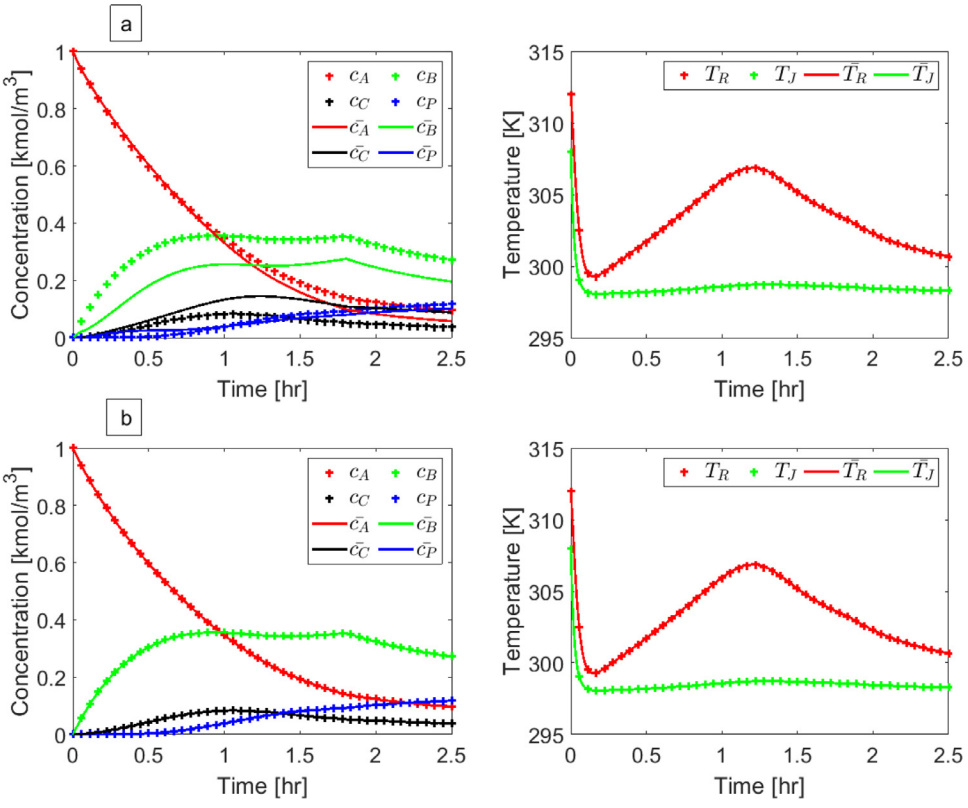


**Fig. 7.** State estimation based on EKF.

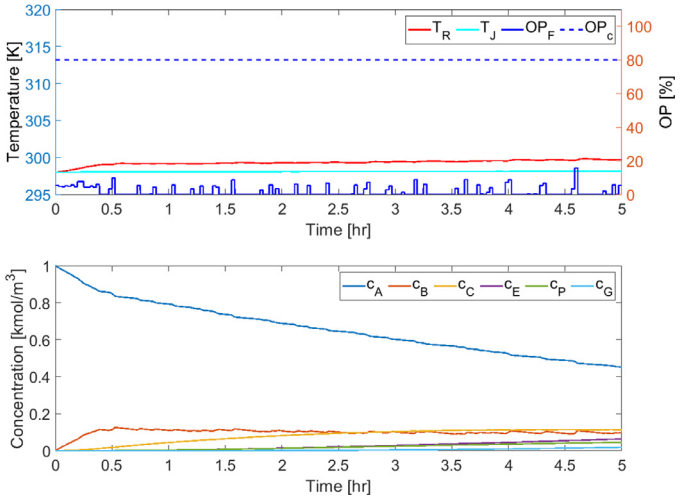


**Fig. 9.** Result of MS-NMPC with nominal kinetic parameters.

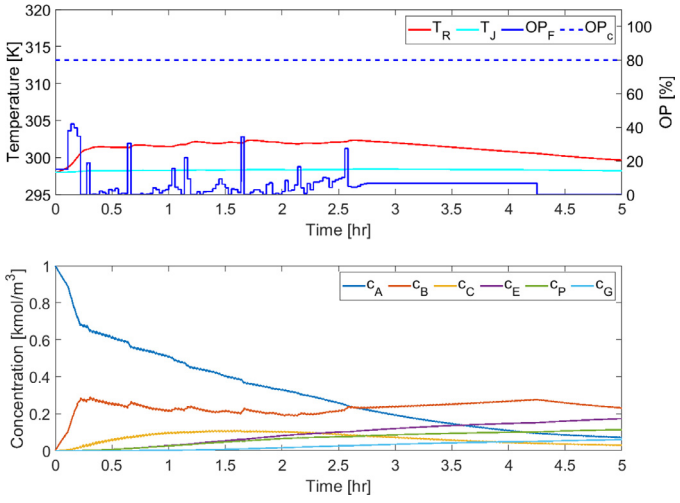


**Fig. 10.** Results of NMPC with respect to the worst case.

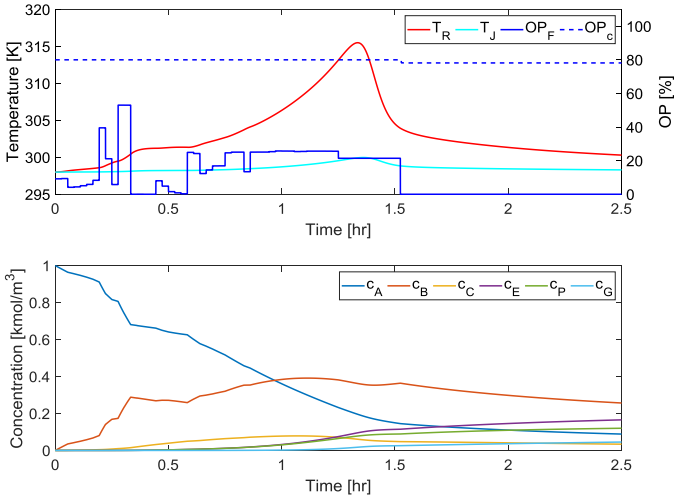


**Fig. 11.** Results of NMPC initialized from the worst-case scenario with updating kinetic parameters.

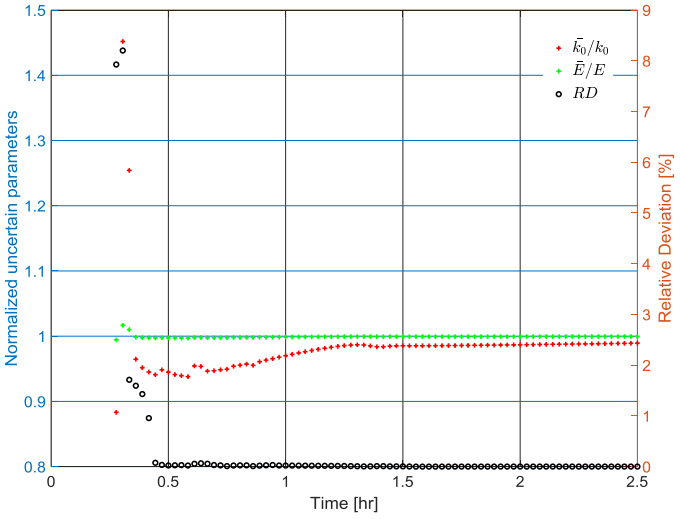


**Fig. 12.** Result of the parameter fitness.

MAT since the applied *MDC* criterion constraints the reactor operation that increases the process safety. At 2.5 h the conversion of component A is 76%, and the yield of P is 37%. The average computational time is 11.5 s per iterations in this case.

### 4.2. Results of the open-loop control under parameter uncertainty

The effect of the parameter uncertainty was analysed using two different algorithms in Sections 4.2.1 and 4.2.2. In the first case, Multi-Stage NMPC was applied, in second case, the worst-case scenario was used to solve the optimization problem under parameter uncertainty. Kinetic parameters of the first reaction ($k_{0,1}$, $E_1$) were chosen as uncertain, where the confidence interval is ±5%. Section 4.2.3 provides the results of the optimization problem when the uncertain parameters are updated iteratively.

#### 4.2.1. Results of Multi-Stage NMPC

The Multi-Stage NMPC algorithm was tested where the uncertain kinetic parameters were changed by 5%. Two uncertain parameters lead to nine scenarios. As shown in Fig. 9, the feed rates are maintained at low values due to the uncertain kinetic parameters. The reason is that the constraints must be satisfied in each scenario, so the development of thermal runaway is avoided in each scenario. Therefore, the results with Multi-Stage NMPC are conservative compared to the nominal solution (Fig. 8). At 2.5 h the conversion of component A is 15.3%, and the yield of P is 2.4%. The average computation time is 660 s per iterations, so real-time optimization is not feasible with the Multi-Stage NMPC algorithm.

#### 4.2.2. Results of the worst-case scenario

The worst case is that the real reaction rate is higher than expected, so in the worst-case scenario, the uncertain pre-exponential factor increases by 5% ($k_{0,1}$ + 5%), and the uncertain activation energy decreases by 5% ($E_1$−5%). The NMPC results are shown in Fig. 10, which naturally is a conservative result. The conversion at 2.5 h is 45%, and the yield of product *P* is 16%. In the worst-case scenario, the average computation time is 17.2 s per iterations, so real-time optimization is feasible with this algorithm.

#### 4.2.3. Worst-case scenario with updating uncertain parameters

The results of the proposed control structure, which was initialized from the worst case, as shown in Fig. 11. With updating uncertain kinetic parameters, the reactor temperature control becomes less conservative and improves the productivity of the operation compared to the worst-case scenario.

At 2.5 h the conversion of component A is 74%, and the yield of P is 36%. Fig. 12 shows the estimated uncertain kinetic parameters; based on the update criterion (Eq. (19) and estimated val-

ues are within the worst case interval) kinetic parameters are first overwritten at 0.61 h. The average computation time is 12.6 s per iterations, hence the real-time optimization is feasible with this algorithm.

Fig. 12 shows how the values of identified kinetic parameters go to the real parameters as more information and measurement is available about the system. Low relative deviations (<1%) indicate that the identified kinetic parameters only slightly change, so we can say that the identified kinetic parameters are near the real system, and we can update the uncertain parameters.

## 5. Conclusion

A framework to keep SBRs with exothermic reactions under control in the whole operation using a nonlinear model predictive control approach is proposed. The framework was tested on the semi-batch version of the Williams-Otto process including three reactions. The proposed control approach can also handle the uncertain kinetic parameters of reactions. In this work, the parameters of the first dominant reaction are considered the source of uncertainty in the model. The proposed framework consists of NMPC, EKF and an identification tool. The Modified Dynamic Condition was implemented into NMPC as an additional safety constraint, and the reactor temperature cannot exceed MAT. EKF is necessary to estimate the state variables of the reactor system and reaction rate constants. Kinetic parameters can be identified with least squares methods based on the estimated reaction constants after some formal transformation.

We have compared the Multi-Stage NMPC solved by the progressive hedging algorithm and worst-case scenario. Each resulted in a conservative solution, but the worst-case scenario NMPC has lower computation time. In the case of MS-NMPC, the size of the optimization problem increases exponentially with the length of the robust horizon and with the uncertain parameters. Therefore, we have decided to extend the worst-case scenario NMPC with the state estimation and identification algorithms. The results show that the proposed approach can handle uncertain kinetic parameters, and can be applied in real reactor systems in which reactor runaway can develop to ensure the optimal production.

Our future investigation will be about implementing the proposed control approach into a lab-scale reactor system.

## Declaration of Competing Interest

The authors declare that they have no known competing financial interests or personal relationships that could have appeared to influence the work reported in this paper.

## CRediT authorship contribution statement

**Alex Kummer:** Conceptualization, Methodology, Software, Formal analysis, Investigation, Writing - original draft, Writing - review & editing, Visualization. **Lajos Nagy:** Conceptualization, Methodology, Writing - review & editing, Supervision. **Tamás Varga:** Conceptualization, Methodology, Writing - review & editing, Supervision.

## Acknowledgement

We would like to express our acknowledgement for the financial support of Széchenyi 2020 under GINOP-2.2.1-15-2017-00059. Tamás Varga's contribution to this paper was supported by the UNKP-19-4 New National Excellence Program of the Ministry for Innovation and Technology.

## References

Abel, O., Helbig, A., Marquardt, W., Zwick, H., Daszkowski, T., 2000. Productivity optimization of an industrial semi-batch polymerization reactor under safety constraints. J. Process Control 10 (Aug. (4)), 351–362. doi:10.1016/S0959-1524(99)00049-9.

Albalawi, F., Durand, H., Christofides, P.D., 2018. Process operational safety via model predictive control: recent results and future research directions. Comput. Chem. Eng. 114, 171–190. doi:10.1016/j.compchemeng.2017.10.006, Jun.

Arellano-Garcia, H., Barz, T., Dorneanu, B., Vassiliadis, V.S., 2020. Real-time feasibility of nonlinear model predictive control for semi-batch reactors subject to uncertainty and disturbances. Comput. Chem. Eng. 133, 106529. doi:10.1016/j.compchemeng.2019.106529, Feb.

Ellis, M., Durand, H., Christofides, P.D., 2014. A tutorial review of economic model predictive control methods. J. Process Control 24 (Aug. (8)), 1156–1178. doi:10.1016/j.jprocont.2014.03.010.

Fabiano, B., Vianello, C., Reverberi, A.P., Lunghi, E., Maschio, G., 2017. A perspective on Seveso accident based on cause-consequences analysis by three different methods. J. Loss Prev. Process Ind. 49, 18–35. doi:10.1016/j.jlp.2017.01.021, Sep.

Findeisen, R., Allgöwer, F., Biegler, L.T.(Eds.), 2007. Assessment and Future Directions of Nonlinear Model Predictive Control, 358. Springer Berlin Heidelberg, Berlin, Heidelberg.

Hall, R.J., "Explosion at T2 Laboratories," 2010. https://www.aiche.org/academy/webinars/explosion-t2-laboratories.

Holtorf, F., Mitsos, A., Biegler, L.T., 2019. Multistage NMPC with on-line generated scenario trees: application to a semi-batch polymerization process. J. Process Control 80, 167–179. doi:10.1016/j.jprocont.2019.05.007, Aug.

Kähm, W., Vassiliadis, V.S., 2018a. Thermal stability criterion integrated in model predictive control for batch reactors. Chem. Eng. Sci. 188, 192–207. doi:10.1016/j.ces.2018.05.032, Oct.

Kähm, W., Vassiliadis, V.S., 2018b. Optimal Lyapunov exponent parameters for stability analysis of batch reactors with Model Predictive Control. Comput. Chem. Eng. 119, 270–292. doi:10.1016/j.compchemeng.2018.08.038, Nov.

Kähm, W., Vassiliadis, V.S., 2019. Thermal stability criterion of complex reactions for batch processes. Chem. Eng. Res. Des. 150, 187–205. doi:10.1016/j.cherd.2019.07.028, Oct.

Kühl, P., Diehl, M., Milewska, A., Molga, E., Bock, H.G., 2007. Robust NMPC for a benchmark fed-batch reactor with runaway conditions. In: Findeisen, R., Allgöwer, F., Biegler, L.T. (Eds.). In: Assessment and Future Directions of Nonlinear Model Predictive Control, 358. Springer Berlin Heidelberg, Berlin, Heidelberg, pp. 455–464.

Kanavalau, A., Masters, R., Kähm, W., Vassiliadis, V.S., 2019. Robust thermal stability for batch process intensification with model predictive control. Comput. Chem. Eng. 130, 106574. doi:10.1016/j.compchemeng.2019.106574, Nov.

Kao, C.-S., Hu, K.-H., 2002. Acrylic reactor runaway and explosion accident analysis. J. Loss Prev. Process Ind. 15 (May (3)), 213–222. doi:10.1016/S0950-4230(01)00070-5.

Khodadadi, H., Jazayeri-Rad, H., 2011. Applying a dual extended Kalman filter for the nonlinear state and parameter estimations of a continuous stirred tank reactor. Comput. Chem. Eng. 35 (Nov. (11)), 2426–2436. doi:10.1016/j.compchemeng.2010.12.010.

Kummer, A., Varga, T., 2017. Feeding trajectory optimization in fed-batch reactor with highly exothermic reactions. Comput. Chem. Eng. 98, 1–11. doi:10.1016/j.compchemeng.2016.12.008, Mar.

Kummer, A., Varga, T., 2019. Completion of thermal runaway criteria: two new criteria to define runaway limits. Chem. Eng. Sci. 196, 277–290. doi:10.1016/j.ces.2018.11.008, Mar.

Kummer, A., Varga, T., Abonyi, J., 2019. Genetic programming-based development of thermal runaway criteria. Comput. Chem. Eng., 106582 doi:10.1016/j.compchemeng.2019.106582, Sep.

Kummer, A., Varga, T., Nagy, L., 2020. Semi-batch reactor control with NMPC avoiding thermal runaway. Comput. Chem. Eng. 134, 106694. doi:10.1016/j.compchemeng.2019.106694, Mar.

Lucia, S., Finkler, T., Engell, S., 2013. Multi-stage nonlinear model predictive control applied to a semi-batch polymerization reactor under uncertainty. J. Process Control 23 (Oct. (9)), 1306–1319. doi:10.1016/j.jprocont.2013.08.008.

Lucia, S., "Robust multi-stage nonlinear modelpredictive control," 2014.

Mayne, D.Q., Seron, M.M., Raković, S.V., 2005. Robust model predictive control of constrained linear systems with bounded disturbances. Automatica 41 (Feb. (2)), 219–224. doi:10.1016/j.automatica.2004.08.019.

Puschke, J., Mitsos, A., 2018. Robust feasible control based on multi-stage eNMPC considering worst-case scenarios. J. Process Control 69, 8–15. doi:10.1016/j.jprocont.2018.07.004, Sep.

Qin, S.J., Badgwell, T.A., 2003. A survey of industrial model predictive control technology. Control Eng. Pract. 11 (Jul. (7)), 733–764. doi:10.1016/S0967-0661(02)00186-7.

Qu, C.C., Hahn, J., 2009. Process monitoring and parameter estimation via unscented Kalman filtering. J. Loss Prev. Process Ind. 22 (Nov. (6)), 703–709. doi:10.1016/j.jlp.2008.07.012.

Rawlings, J.B., Mayne, D.Q., 2009. Model Predictive Control: Theory and Design. Wis: Nob Hill Pub, Madison.

Rossi, F., Copelli, S., Colombo, A., Pirola, C., Manenti, F., 2015. Online model-based optimization and control for the combined optimal operation and runaway prediction and prevention in (fed-)batch systems. Chem. Eng. Sci. 138, 760–771. doi:10.1016/j.ces.2015.09.006, Dec.

Rossi, F., Reklaitis, G., Manenti, F., Buzzi-Ferraris, G., 2016. Multi-scenario robust online optimization and control of fed-batch systems via dynamic model-based scenario selection. AIChE J. 62 (Sep. (9)), 3264–3284. doi:10.1002/aic.15346.

Rossi, F., Manenti, F., Pirola, C., Mujtaba, I., 2016. A robust sustainable optimization & control strategy (RSOCS) for (fed-)batch processes towards the low-cost reduction of utilities consumption. J. Clean. Prod. 111, 181–192. doi:10.1016/j.jclepro.2015.06.098, Jan.

Rossi, F., Manenti, F., Buzzi-Ferraris, G., Reklaitis, G., 2017. Combined dynamic optimization, optimal control and online runaway detection prevention under uncertainty. Chem. Eng. Trans. 57, 973–978. doi:10.3303/CET1757163, 0.

Schweitzer, J.-M., López-García, C., Ferré, D., 2010. Thermal runaway analysis of a three-phase reactor for LCO hydrotreatment. Chem. Eng. Sci. 65 (Jan. (1)), 313–321. doi:10.1016/j.ces.2009.07.012.

Scokaert, P.O.M., Mayne, D.Q., 1998. Min-max feedback model predictive control for constrained linear systems. IEEE Trans. Automat. Control 43 (Aug. (8)), 1136–1142. doi:10.1109/9.704989.

Seki, H., Ogawa, M., Ooyama, S., Akamatsu, K., Ohshima, M., Yang, W., 2001. Industrial application of a nonlinear model predictive control to polymerization reactors. Control Eng. Pract. 9 (Aug. (8)), 819–828. doi:10.1016/S0967-0661(01)00046-6.

Sriram, M., Stevens, W.F., 1973. An example of the application of nonlinear programming to chemical-process optimization. Oper. Res. 21 (1), 296–304. doi:10.1287/opre.21.1.296, Feb.

Thangavel, S., Lucia, S., Paulen, R., Engell, S., 2018. Dual robust nonlinear model predictive control: a multi-stage approach. J. Process Control 72, 39–51. doi:10.1016/j.jprocont.2018.10.003, Dec.

van Woezik, B.A.A., Westerterp, K.R., 2000. The nitric acid oxidation of 2-octanol. A model reaction for multiple heterogeneous liquid–liquid reactions. Chem. Eng. Process. 39 (Nov. (6)), 521–537. doi:10.1016/S0255-2701(00)00099-4.

Vanderbei, R.J., Shanno, D.F., 1999. An interior-point algorithm for nonconvex nonlinear programming. Comput. Optim. Appl. 13 (1/3), 231–252. doi:10.1023/A:1008677427361.

Westerterp, K.R., Molga, E.J., 2004. No more runaways in fine chemical reactors. Ind. Eng. Chem. Res. 43 (Aug. (16)), 4585–4594. doi:10.1021/ie030725m.

Yu, Z.J., Biegler, L.T., 2019. Advanced-step multistage nonlinear model predictive control: robustness and stability. J. Process Control 84, 192–206. doi:10.1016/j.jprocont.2019.10.006, Dec.

Zhang, Z., Wu, Z., Durand, H., Albalawi, F., Christofides, P.D., 2018. On integration of feedback control and safety systems: analyzing two chemical process applications. Chem. Eng. Res. Des. 132, 616–626. doi:10.1016/j.cherd.2018.02.009, Apr.

Zhang, B., Hou, H., Hao, L., Zhu, J., Sun, Y., Wei, H., 2019. Identification and optimization of thermally safe operating conditions for single kinetically controlled reactions with arbitrary orders in isoperibolic liquid-liquid semibatch reactors. Chem. Eng. J. 375, 121975. doi:10.1016/j.cej.2019.121975, Nov.